IIETA International Information and Engineering Technology Association
Advancing the World of Information and Engineering

Journal Européen des Systèmes Automatisés
Vol. 59, No. 7, July, 2026, pp. 2037-2048
Journal homepage: http://iieta.org/journals/jesa

Asymmetric Leader-Follower Sine Cosine Algorithm for Global Maximum Power Point Tracking in Photovoltaic Systems under Dynamic Partial Shading

N. M. Nasir[1], Nor Maniha Abdul Ghani[1*], Kamal Z. Zamli[2], Mohammad Osman Tokhi[3]

[1] Faculty of Electrical and Electronics Engineering Technology, Universiti Malaysia Pahang Al-Sultan Abdullah, Pekan 26600, Malaysia
[2] Faculty of Computing, Universiti Malaysia Pahang Al-Sultan Abdullah, Pekan 26600, Malaysia
[3] School of Engineering, London South Bank University, London SE10AA, UK

Corresponding Author Email: normaniha@umpsa.edu.my

https://doi.org/10.18280/jesa.590719

Received: 11 May 2026
Revised: 4 July 2026
Accepted: 21 July 2026
Available online: 31 July 2026

Keywords:
maximum power point tracking, photovoltaic systems, partial shading conditions, Sine Cosine Algorithm, asymmetric leader–follower optimisation, metaheuristic optimisation

ABSTRACT

Partial shading conditions (PSCs) create multiple local maximum power points (LMPPs) that reduce the effectiveness of conventional maximum power point tracking (MPPT) algorithms in photovoltaic (PV) systems. Although the Sine Cosine Algorithm (SCA) has demonstrated promising global search capability, its identical stochastic updates for all search agents often result in excessive population diversity, slower convergence, and steady-state oscillations. This paper proposes an Asymmetric Leader–Follower Sine Cosine Algorithm (ALF-SCA) for global MPPT under dynamic PSCs. The proposed framework integrates asymmetric leader–follower coordination, global-best anchoring, convergence locking, and environmental reinitialisation while preserving the original exploration–exploitation mechanism of SCA. The algorithm was evaluated under uniform dynamic irradiance and two dynamic partial shading scenarios, and compared with the conventional SCA, Particle Swarm Optimisation (PSO), Whale Optimisation Algorithm (WOA), Harris Hawks Optimisation (HHO), and Perturb and Observe (PO) algorithm. Simulation results demonstrate that ALF-SCA consistently achieved tracking efficiencies above 99%, reduced cumulative tracking error, and improved convergence stability under increasingly complex shading conditions. Furthermore, the proposed method preserves the same theoretical computational complexity as the conventional SCA while introducing only a marginal increase in execution latency, indicating that the improved tracking performance is achieved with minimal additional computational overhead.

1. INTRODUCTION

Partial shading conditions (PSCs) remain one of the primary challenges affecting the energy harvesting capability of photovoltaic (PV) systems. Under PSCs, bypass diode activation produces multiple local maximum power points (LMPPs) on the power-voltage (P-V) characteristic, increasing the likelihood that conventional maximum power point tracking (MPPT) algorithms converge to suboptimal operating points [1]. Consequently, significant energy losses may occur under rapidly changing environmental conditions, motivating the development of more robust global maximum power point tracking (GMPPT) techniques [2, 3].

Conventional MPPT methods, including Perturb and Observe (PO) [4-6] and Incremental Conductance (INC) [7, 8], remain attractive because of their simplicity and low computational requirements. However, their hill-climbing search mechanism is inherently susceptible to becoming trapped at local optima under PSCs. Recent improvements based on adaptive step-size control have enhanced transient performance under varying irradiance but generally remain ineffective in multimodal P-V characteristics [9]. Consequently, intelligent MPPT approaches have attracted increasing attention because of their ability to perform global optimisation under complex operating conditions [10, 11].

Recent intelligent MPPT research has expanded beyond conventional optimisation by incorporating fuzzy logic [12], machine learning [13], and population-based metaheuristic algorithms [14]. Artificial intelligence approaches, including adaptive neuro-fuzzy and deep learning models [15, 16], have demonstrated improved adaptability to nonlinear PV behaviour and dynamically adjust optimisation parameters to improve convergence under rapidly changing irradiance [15, 17]. Despite these advances, many intelligent approaches require extensive computational resources or complex training procedures, limiting their suitability for real-time embedded MPPT applications.

Meanwhile, population-based metaheuristics have also become a recent trend in developing GMPPT to search for global optima or the global peak of P-V curve of PV array that is subjected to PSCs. These multi-agent optimisation techniques, including Particle Swarm Optimisation (PSO) MPPT [18-20], Grey Wolf Optimizer (GWO) [21-23], and Sine Cosine Algorithm (SCA) [24-27], simulate biological or physical processes to identify the global maximum power point (GMPP) across multi-peak P-V curves. Unlike the single-point search of PO, they distribute multiple agents throughout the operating range to facilitate communication and movement toward the most promising regions. This collective intelligence enables the system to bypass local maxima, as population diversity increases the probability of discovering the global peak during severe shading events.

However, practical deployment of intelligent MPPT algorithms requires careful consideration of embedded hardware limitations [17, 27]. Recent implementations using digital signal processors (DSPs), field-programmable gate arrays (FPGAs), and hardware-in-the-loop (HIL) platforms have demonstrated that execution latency and computational complexity directly influence real-time tracking capability [27, 28]. Consequently, recent research has increasingly focused on lightweight adaptive optimisation techniques that maintain high tracking performance without imposing excessive computational overhead [17, 27].

Among existing metaheuristic approaches, the SCA [29] has attracted considerable attention because of its simple mathematical formulation, tuning-free, and low computational complexity. Unlike other algorithms that require many tuning parameters, such as PSO with two tuning parameters and Genetic Algorithm (GA) with four tuning parameters [30], SCA, by default, focuses only on the number of populations to be used. Nevertheless, the standard SCA applies identical stochastic update rules to all search agents throughout the optimisation process [25]. Although this promotes exploration, excessive population diversity may persist during the exploitation stage, resulting in slower convergence and increased steady-state oscillations. Furthermore, the standard SCA as most standard metaheuristics, lacks an explicit mechanism to distinguish optimisation convergence from environmental changes [31], reducing its adaptability under dynamic PSCs. These limitations motivate the development of a modified optimisation framework capable of improving convergence stability while preserving the computational efficiency of the original SCA.

To address these limitations, this paper proposes an Asymmetric Leader-Follower Sine Cosine Algorithm (ALF-SCA) for GMPPT under dynamic PSCs. Rather than modifying a single search component, the proposed framework integrates asymmetric leader-follower coordination, global-best anchoring, convergence locking, and environmental reinitialisation into a unified optimisation strategy. These complementary mechanisms improve the balance between exploration and exploitation while maintaining computational efficiency for real-time MPPT applications. Despite recent advances in intelligent MPPT, existing SCA-based approaches generally do not integrate asymmetric search coordination, convergence control, and environmental reinitialisation within a unified optimisation framework for dynamic PSCs. The main contributions of the proposed ALF-SCA are:

- An ALF-SCA is proposed for GMPPT under dynamic PSCs. Unlike the conventional SCA, the proposed framework assigns complementary search roles to the leader and follower agents to improve the balance between global exploration and local exploitation during the optimisation process.
- A coordinated optimisation framework integrating global-best anchoring, convergence locking, and environmental reinitialisation is developed to accelerate convergence, suppress unnecessary steady-state oscillations, and enable rapid re-tracking following significant irradiance changes while preserving the computational simplicity of the original SCA.
- A comprehensive performance evaluation is conducted under progressively challenging operating conditions, including uniform dynamic irradiance and two dynamic partial shading scenarios with multiple local maxima. The proposed ALF-SCA is benchmarked against conventional PO and representative metaheuristic MPPT algorithms, namely SCA, PSO, Whale Optimisation Algorithm (WOA), and Harris Hawks Optimisation (HHO), using tracking efficiency, convergence time, and the integral of time-weighted squared error (ITSE).
- The practical feasibility of the proposed framework is verified through computational complexity and execution latency analyses, demonstrating that the improved tracking performance is achieved with only a marginal increase in execution latency while maintaining the same theoretical computational complexity as the original SCA, supporting its suitability for real-time embedded MPPT applications.

The rest of the paper is configured as follows. Section 2 is the electrical characteristics of the PV and the system configuration in this study. Section 3 formulates the problem regarding the SCA-MPPT, while Section 4 introduces the proposed ALF-SCA. Section 5 details the simulation preparation. Section 6 presents the performance results, including dynamic tracking evaluations and a computational complexity analysis, while Section 7 provides a detailed discussion of the findings. Finally, Section 8 presents the concluding remarks.

2. PHOTOVOLTAIC SYSTEM

To simulate the non-linear electrical output of the PV array under uniform and PSCs, the standard single-diode model is adopted [32]. The terminal current (I) generated by the PV array is governed by Eq. (1).

$$\mathrm{I} = I_{ph} - I_0\left[exp\left(\frac{q(V+IR_s)}{nkT}\right)-1\right]-\frac{V+IR_s}{R_{sh}} \tag{1}$$

where, I_{ph} represents the light-generated photocurrent, I_0 is the reverse saturation current of the diode, q is the electron charge (1.602×10^{-19} C), k is the Boltzmann constant (1.381×10^{-23} J/K), T is the p-n junction temperature in Kelvin, and n is the diode ideality factor. The parameters R_s and R_{sh} denote the equivalent series and parallel resistance of the array, respectively.

A PV model, SunPower SPR-215 PV module, was utilized to simulate the various test cases in this study, including uniform irradiance and partial shading under a dynamic environmental configuration. Table 1 shows the specifications of the PV module at Standard Test Condition (STC). In this study, the module operating temperature is fixed at 25 °C.

Table 1. SPR-215 module specification at standard test condition

PV Module Parameters at STC	Configuration
PV maximum power, P_{mp}	214.92 W
Voltage at MPP, V_{mp}	39.8 V
Current at MPP, I_{mp}	5.4 A
Open Circuit Voltage, V_{oc}	48.3 V
Short Circuit Current, I_{sc}	5.8 A

Note: PV = photovoltaic, STC = Standard Test Condition.

A DC-DC boost converter was utilized to enable DC control by the MPPT algorithm to adjust the operating voltage with the controlled PWM signal by controlling the duty cycle value. The parameter configurations were given as in Table 2. The MPPT controlled the duty cycle at a fixed rate of 15 ms to account for stable transient feedback of the DC converter.

Table 2. Specification of DC-DC boost converter

Parameter	Configuration
Inductor, L	33.00 mH
Input Capacitor, C_{in}	1 μF
Output Capacitor, C_{out}	8.4 μF
Switching Frequency, f_{sw}	20 kHz
Resistor Load, R	540 Ω

3. PROBLEM FORMULATION OF SINE COSINE ALGORITHM MPPT

The SCA, proposed by Mirjalili, is a population-based metaheuristic technique that simulates trigonometric behavior to oscillate candidate solutions toward a target vector [29]. Position updates are governed by Eqs. (2) and (3).

$$x_k^{t+1} = \begin{cases} x_k^t + r_1 \sin(r_2) \cdot |r_3 x^* - x_k^t|, & \text{if } r_4 < 0.5 \\ x_k^t + r_1 \cos(r_2) \cdot |r_3 x^* - x_k^t|, & \text{else} \end{cases} \quad (2)$$

$$r_1 = a - a\frac{t}{T} \quad (3)$$

where, x_k^{t+1} represents the updated position, x_k^t is the current position of agent k, and x^* is the current best position. The stochastic parameter $r_2 \in [0, 2\pi]$ determines the movement direction, $r_3 \in [0, 2]$ acts as a destination weight, and $r_4 \in [0, 1]$ dictates the choice between sine and cosine transitions. The control parameter r_1 linearly decays from a to 0 over the maximum iterations T to transition the search from exploration to exploitation.

Various SCA-based MPPT have been reported in recent literature, showing improved PV power performance [24, 25]. These studies proposed that the duty cycle control of the PV system is directly optimized by the SCA, with the algorithm's populations or agents serving as the operating duty cycle, d_k^t. The SCA MPPT can be redefined as in Eq. (4).

$$d_k^{t+1} = \begin{cases} d_k^t + r_1 \sin(r_2) \cdot |r_3 d^* - d_k^t|, & \text{if } r_4 < 0.5 \\ d_k^t + r_1 \cos(r_2) \cdot |r_3 d^* - d_k^t|, & \text{else} \end{cases} \quad (4)$$

Recent SCA-based MPPT studies have commonly modified the original SCA by fixing the destination weight ($r_3 = 1$) while simultaneously replacing the linearly decreasing control parameter r_1 with a uniformly distributed random variable [25]. These modifications have been reported to improve MPPT performance under PSCs. However, the underlying optimisation rationale remains insufficiently justified. In the original SCA, the linear decay of r_1 explicitly governs the transition from exploration to exploitation and progressively reduces the search amplitude until convergence at the maximum iteration. Replacing r_1 with a random variable removes this deterministic transition, transforming the parameter from an exploration–exploitation controller into a purely stochastic search factor. Consequently, the optimisation process is no longer explicitly guided toward convergence, and its relationship with the predefined maximum iteration becomes less well defined. Although improved MPPT performance has been reported, the mechanisms responsible for these improvements remain largely unexplained in the existing literature.

Although standard implementation of $r_3 \in [0, 2]$ introduces arbitrary scaling that alters updating step sizes without accounting for physical convergence stages, eliminating r_3 from the optimisation framework may also reduce exploration capability during the early optimisation stages, increasing the possibility of premature convergence under multimodal PV power curves.

Previous SCA-MPPT modifications improved performance empirically but altered the theoretical role of the exploration–exploitation controller without sufficient justification. ALF-SCA preserves the original optimisation philosophy while redesigning the coordination between search agents.

4. THE PROPOSED ASYMMETRIC LEADER-FOLLOWER SINE COSINE ALGORITHM

To overcome the limitations identified in Section 3, the proposed ALF-SCA introduces a coordinated optimisation framework for dynamic MPPT. Rather than altering the fundamental mathematical structure of the original SCA, the proposed method selectively redesigns the search coordination mechanism through four complementary components: linear agent initialisation, asymmetric leader–follower updates, convergence locking, and environmental reinitialisation. These components operate collectively to improve exploration–exploitation balance, suppress steady-state oscillations, and maintain rapid adaptation under dynamic PSCs. In this study, the objective of the optimisation is to maximize the PV power $P(t)$ output.

4.1 Initialization of search agents

The optimisation process begins by linearly distributing three search agents N across the predefined duty-cycle search space, denoted as $d_k = \{d_1, d_2, d_3\} = \{0.2, 0.5, 0.8\}$. Linear initialization provides uniform coverage of the feasible operating region bounded between $d_{\min} = 0.1$ and $d_{\max} = 0.9$ to ensure the boost converter operates within continuous conduction mode while covering potential local peaks across the P-V curve under PSCs. Since each search agent directly represents a converter duty cycle, these boundaries also prevent infeasible switching commands during the optimisation process.

4.2 Asymmetrical role of leader and follower around the global best position

To address population dispersion, the proposed method replaces individual-agent reference points with the global-best position, d^*. Referencing all position updates to the current global-best solution directs the population towards a common optimisation target, preventing individual agents from drifting away during the later optimisation stages. Furthermore, because the candidate agents are uniformly initialised across known physical duty-cycle boundaries, the original linear decay parameter r_1 is retained to preserve the gradual transition from exploration to exploitation established in the conventional SCA.

Unlike conventional SCA, where every search agent follows identical stochastic update rules, the proposed ALF-SCA assigns complementary search responsibilities to the leader and follower agents. During each optimisation iteration, the candidate producing the highest PV power is designated as the leader and continues performing exploratory movement around the current global-best solution. To preserve the original exploration capability of SCA, the leader retains the stochastic destination weight $r_3 \in [0,2]$, allowing controlled local exploration around the most promising operating point while maintaining the possibility of escaping nearby local optima under complex PSCs. The leader position is therefore updated according to Eq. (5).

$$d_{\text{leader}}^{t+1} = \begin{cases} d_{\text{leader}}^{t} + r_1 \sin(r_2) \cdot |r_3 d^* - d_{\text{leader}}^{t}|, & \text{if } r_4 < 0.5 \\ d_{\text{leader}}^{t} + r_1 \cos(r_2) \cdot |r_3 d^* - d_{\text{leader}}^{t}|, & \text{else} \end{cases} \quad (5)$$

Conversely, the remaining agents designated as follower agents use a fixed unity weight ($r_3 = 1.0$). Setting $r_3 = 1.0$ eliminates directional ambiguity in step size, pulling follower agents directly toward the global-best position to form a tight population cluster by the final iteration. The update equation for follower agents (while $k \neq$ leader) is given by Eq. (6).

$$d_k^{t+1} = \begin{cases} d^* + r_1\, sin(r_2) \times |d^* - d_k^t|, & if\ r_4 \leq 0.5 \\ d^* + r_1\, cos(r_2) \times |d^* - d_k^t|, & else \end{cases} \quad (6)$$

4.3 Convergence criteria and environmental changes detection

To prevent steady-state power oscillations and ensure convergence, the algorithm evaluates duty cycle diversity across the population using Eq. (7). When the population diversity Δd_{th} drops below 0.001, the MPPT hold to the optimal duty cycle (d^*), entering a convergence state.

$$\Delta d_{\text{th}} = \max(d_k^t) - \min(d_k^t) \quad (7)$$

Additionally, to guarantee convergence, the MPPT utilizes the maximum iteration-based criteria, where T = 20. Under a population size of 3, the proposed ALF-SCA would execute a 60-sampling evaluation for MPPT optimisation and execute the d^* value continuously to the converter where the agent's solution is concluded.

While in convergence state, the proposed MPPT incorporates continuous environmental monitoring during steady state, sampling the PV power $P(t)$, PV voltage $V(t)$, and PV current $I(t)$. Continuous sampling is crucial to ensure the proposed MPPT able to adapt to environmental changes that cause sudden shift in PV power.

The adaptation mechanism of the proposed ALF-SCA utilized power variation ratio, P_{ratio}, and evaluated alongside the directional changes of voltage (ΔV) and current (ΔI). The expression of the two conditional adaptations can be written as in Eqs. (8) and (9).

$$P_{\text{ratio}} = \frac{|P_{G\text{best}} - P(t)|}{P_{G\text{best}}} \quad (8)$$

$$\Delta V = V_{\text{best}} - V(t), \qquad \Delta I = I_{\text{best}} - I(t) \quad (9)$$

where, $P_{G\text{best}}$ is the global-best of PV power found at convergence, while V_{best} and I_{best} are the recorded voltage and current of the PV power at convergence respectively.

An environmental change is confirmed when the P_{ratio} exceeds a threshold of 5%, which is consistent with various literature [11, 33-35]. The mathematical basis of this threshold stems directly from the single-diode PV formulation presented in Eq. (1), where the I_{ph} scales in direct linear proportional to solar irradiance ($I_{ph} \propto G$). As a result, any step change in solar irradiance G induces an almost identical percentage variation in array output power. Based on the sensitivity analysis conducted in this study, a value of 5% is adequate to reliably detect any power shift by solar irradiance changes.

Furthermore, in this study, the electrical measurements fed to the MPPT are filtered out for any high-frequency transient feedback and sensor measurement noises. Upon detection, the proposed MPPT reinitializes the population across the search space to track the new global peak.

Algorithm 1: Asymmetric Leader-Follower Sine Cosine Algorithm (ALF-SCA) Maximum Power Point Tracking (MPPT)

Input: Array Voltage $V(t)$, Current $I(t)$, Parameters (N, T, a, $d_{\min}$, $d_{\max}$)
Output: Converter Operating Duty Cycle d_{out}
1: Linearly distribute candidate agents: $d_k \in [d_{\min}, d_{\max}]$ for $k = 1, \ldots, N$
2: Set iteration count $t = 1$, sample index $k = 1$, $P_{\text{Gbest}} = 0$
3: Calculate present power $P(t) = V(t) \times I(t)$

4: **if** $P(t) > P_{\text{Gbest}}$ **then**
5: Update $P_{\text{Gbest}} = P(t)$, $V_{\text{best}} = V(t)$, $I_{\text{best}} = I(t)$, $d^* = d_k^t$
6: end if

7: Identify Leader Agent: $d_{\text{leader}}^t = d^*$
8: **for** each agent $k = 1$ to N **do**
9: Generate random parameters**:** $r_2 \in [0, 2\pi]$, $r_4 \in [0, 1]$
10: **if** agent k is Leader ($d_k^t == d_{\text{leader}}^t$) **then**
11: Select stochastic weight $r_3 \in [0, 2]$
12: Compute updated position d_{leader}^{t+1} using Eq. (5)
13: else
14: Set followers' weight $r_3 = 1.0$
15: Compute updated follower position d_k^{t+1} using Eq. (6)
16: end if
17: end for

18: Calculate population diversity Δd_{th} using Eq. (7)
19: **if** $\Delta d_{\text{th}} < 0.001$ **OR** $t \geq T$ **then**
20: **return** $d_{\text{out}} = d^*$
21: end if

22: Calculate power ratio P_{ratio} using Eq. (8) alongside $\Delta V, \Delta I$ using Eq. (9)
23: **if** Change criteria satisfied (P_{ratio} > 5%) **AND** directional shifts met **then**
24: Go to Line 1
25: end if

26: $t = t + 1$

4.4 Algorithm overview

To provide a clear structural overview of the operational logic for digital implementation, the complete step-by-step workflow of the proposed ALF-SCA MPPT is synthesized in Algorithm 1. The pseudocode illustrates the seamless transition between active tracking, leader-follower update mechanics, steady-state convergence locking, and environmental reset triggers, directly referencing the mathematical formulations in Eqs. (5)-(9).

4.5 Qualitative verification of the proposed search mechanism

Before evaluating the proposed ALF-SCA under PV operating conditions, a qualitative verification was conducted to examine whether the proposed search coordination mechanism behaves as intended. The Schwefel 2.26, F_8 benchmark function [36], was selected because of its highly multimodal optimisation landscape containing numerous local optima, making it suitable for visualising the exploration and exploitation characteristics of population-based optimisation algorithms. Unlike the PV optimisation problem, which is influenced by converter dynamics and environmental variations, the benchmark function provides a controlled optimisation environment for directly observing the search behaviour of the proposed algorithm.

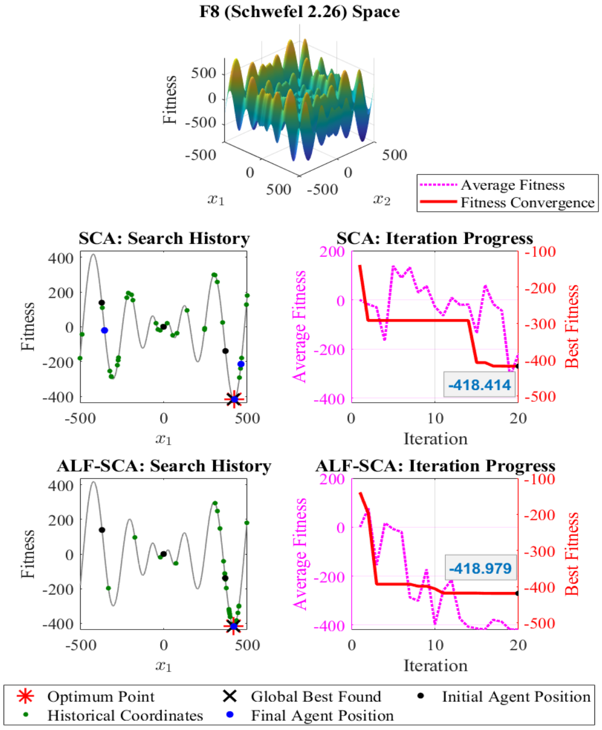

Figure 1. Qualitative comparison of search mechanics between standard SCA and proposed ALF-SCA on the multimodal F_8 (Schwefel 2.26) benchmark function ($N = 3$, $T = 20$, $D = 1$)

Note: SCA= Sine Cosine Algorithm, ALF-SCA = Asymmetric Leader-Follower Sine Cosine Algorithm.

Both the conventional SCA and the proposed ALF-SCA were evaluated using identical initial population distributions and optimisation parameters to ensure a fair comparison. Figure 1 illustrates the search trajectories of the optimisation agents throughout the optimisation process, where the coloured markers represent the agent positions and the global optimum corresponds to the known optimum of the Schwefel function.

The conventional SCA maintains stochastic movement for all search agents throughout the optimisation process, resulting in a relatively dispersed population even during the later optimisation stages. Although this behaviour promotes exploration, excessive population diversity delays convergence towards the global optimum and increases trajectory fluctuations around promising regions.

In contrast, the proposed ALF-SCA initially preserves sufficient exploration through stochastic leader movement while progressively reducing population dispersion via deterministic follower coordination. As the optimisation progresses, the follower population contracts towards the leader, producing a coordinated search pattern around the global-best solution. Consequently, all search agents converge towards the global optimum with substantially reduced population dispersion while maintaining sufficient exploratory capability during the early optimisation stage.

The observed search behaviour provides qualitative evidence that the proposed asymmetric leader–follower coordination successfully balances exploration and exploitation without modifying the original optimisation philosophy of the SCA. These observations support the design rationale presented in Section 4.2 and provide the theoretical basis for the PV MPPT performance evaluation presented in Section 6.

5. SIMULATION PREPARATION AND TESTING CONFIGURATION

The proposed ALF-SCA was evaluated in MATLAB R2024a using a detailed PV system comprising a 12-module series-connected PV array as in Figure 2 and the DC–DC boost converter specified in Table 2. The MPPT controller operated at a fixed sampling interval of 15 ms, allowing sufficient converter settling time between successive duty-cycle.

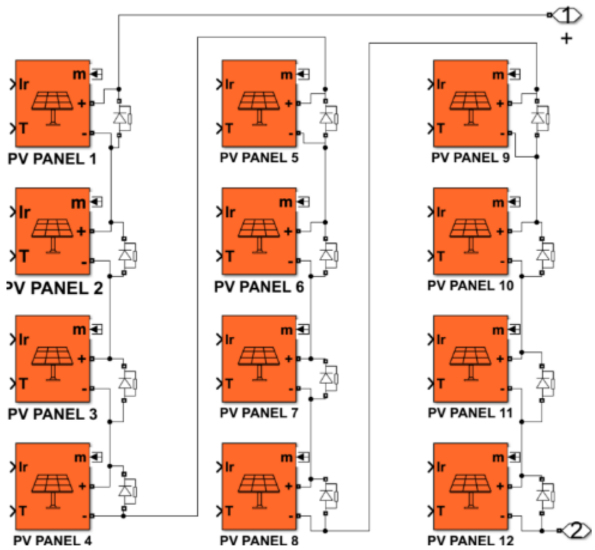

Figure 2. Photovoltaic (PV) array configuration

To assess the performance of the ALF-SCA MPPT, the proposed algorithm was tested and compared across several test cases with dynamic irradiance and partial shading. Three dynamic test cases were used: uniform dynamic irradiance condition (UDC), dynamic partial shading case 1 (DPSC1), and dynamic partial shading case 2 (DPSC2). The dynamic cases have a sequence of test cases, and each sequence runs for 1.5 seconds before shifting to the next case.

The UDC consists of three irradiance transitions: 1000 W/m², 800 W/m², and 400 W/m², each applied uniformly across all 12 PV modules. Figure 3 presents the corresponding $P-V$ characteristics, where the GMPP decreases from 2565.446 W to 2063.617 W and finally to 1032.285 W following the irradiance reduction.

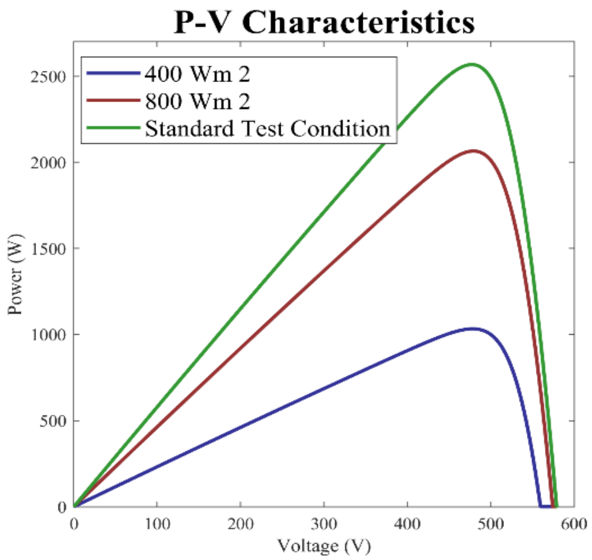

Figure 3. Power-voltage (P-V) characteristic under uniform dynamic condition (UDC)

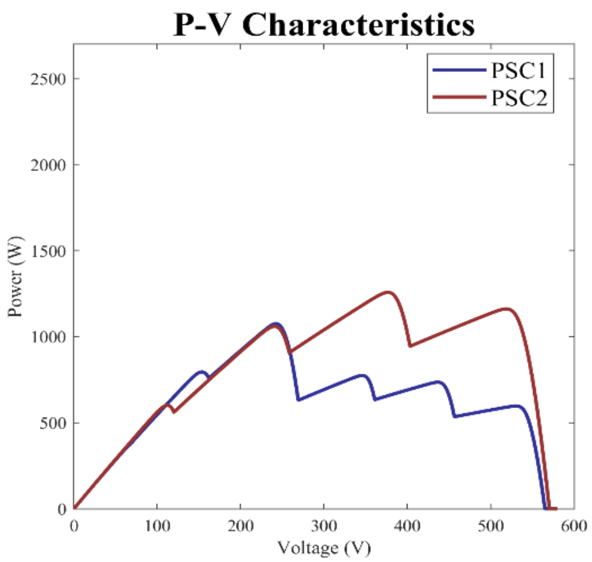

Figure 4. Power-voltage (P-V) characteristic of uniform irradiances of dynamic partial shading case 1 (DPSC1)

Dynamic partial shading was evaluated using two increasingly challenging scenarios, namely DPSC1 and DPSC2. DPSC1 consists of two irradiance transitions (PSC1 and PSC2), where the algorithms must identify the GMPPs of 1074.516 W and 1256.620 W despite the presence of multiple local maxima. DPSC2 presents a more demanding evaluation comprising PSC3 and PSC4. PSC3 contains closely spaced power peaks with a GMPP of 1985.441 W, whereas PSC4 produces twelve distinct local maxima with a GMPP of 924.939 W. The corresponding P-V characteristics are illustrated in Figures 4 and 5.

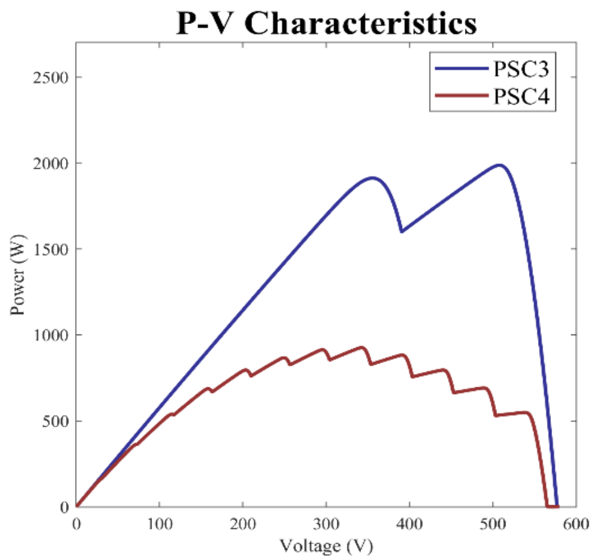

Figure 5. Power-voltage (P-V) characteristic of uniform irradiances of dynamic partial shading case 2 (DPSC2)

6. RESULTS

The proposed ALF-SCA was evaluated under three operating scenarios with progressively increasing complexity to assess its tracking performance under dynamic environmental conditions. The evaluation began with uniform dynamic irradiance (UDC), followed by two dynamic partial shading scenarios (DPSC1 and DPSC2) that introduced multiple LMPPs and rapidly changing irradiance patterns. The proposed method was compared with the original SCA, PSO, WOA, HHO, and the conventional PO algorithm. For stochastic optimisation algorithms, statistical performance was obtained from 30 independent simulation runs, while PO was evaluated deterministically. Tracking efficiency, convergence time, and the ITSE were used to assess tracking accuracy, transient response, and overall control performance. Table 3 shows the parameters used in this study. All competing algorithms use a configuration of N = 3 and T = 20.

Table 3. Algorithms' parameters configuration

Algorithms	Tuning Parameters
Proposed ALF-SCA	–
SCA [29]	–
PSO [37]	Inertia weight, w = 0.4, cognitive coefficient, c_1 = 1.2, and social coefficient, c_2=1.5
WOA [38]	Spiral constant, b = 1
HHO [39]	–
PO	Step size, Δd = 0.05

Note: *The "-" indicates no tuning parameter involves. ALF-SCA = Asymmetric Leader-Follower Sine Cosine Algorithm, SCA = Sine Cosine Algorithm, PSO = Particle Swarm Optimisation, WOA = Whale Optimisation Algorithm, HHO = Harris Hawks Optimisation, PO = Perturb and Observe.

6.1 Performance under uniform dynamic irradiance

The first evaluation considers uniform irradiance conditions to establish the baseline performance of the proposed controller under a single-MPP operating environment. The irradiance was sequentially changed from 1000 W/m² to 800 W/m² and subsequently to 400 W/m², corresponding to theoretical maximum power values of 2565.45 W, 2063.62 W, and 1032.29 W, respectively.

Figure 6 shows that all metaheuristic-based controllers successfully tracked the MPP under the three irradiance levels, whereas PO exhibited the expected hill-climbing response. Nevertheless, clear differences were observed during convergence. The original SCA produced persistent power oscillations before reaching steady state, while WOA and HHO required longer settling periods after each irradiance transition. In contrast, ALF-SCA converged smoothly towards the new operating point and maintained a stable output throughout the remaining operating interval.

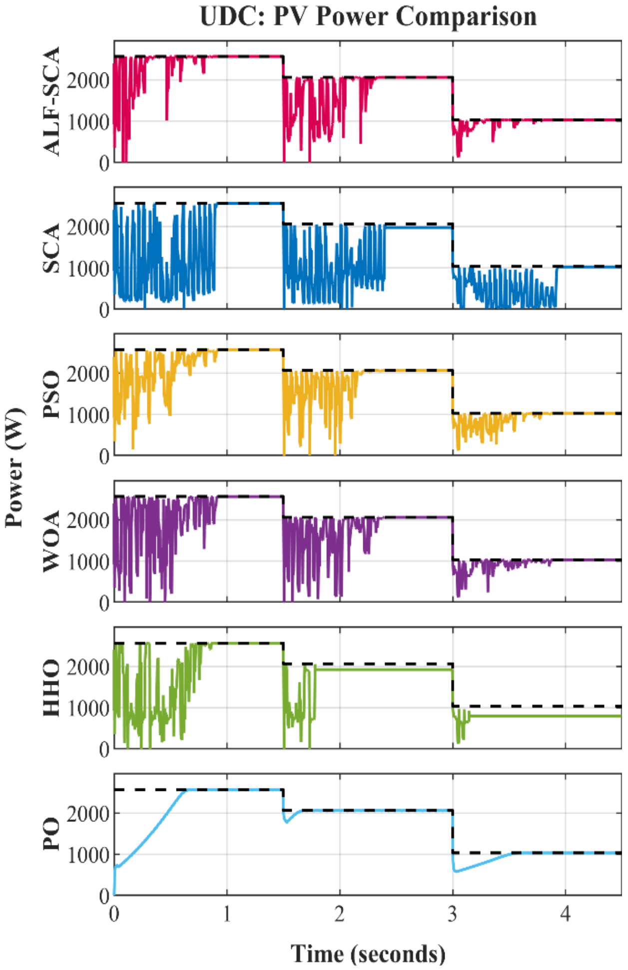

Figure 6. Photovoltaic (PV) power tracking comparison under uniform dynamic condition (UDC) step transitions (1000 W/m^2 → 800 W/m^2 → 400 W/m^2)

The statistical results in Table 4 confirm these observations. ALF-SCA maintained tracking efficiencies exceeding 99% under all irradiance levels, with mean efficiencies of 99.19 ± 3.25%, 99.71 ± 0.67%, and 99.14 ± 3.76% for 1000, 800, and 400 W/m², respectively. More importantly, the proposed controller consistently achieved substantially lower ITSE values than the original SCA, reducing the cumulative tracking error from 88.67 ± 38.69 to 6.96 ± 4.59 under the initial operating condition. Overall, the proposed controller establishes a stable baseline under single-GMPP conditions, demonstrating that its convergence behaviour remains effective even during successive irradiance transitions.

While all evaluated algorithms achieved high tracking efficiencies under uniform irradiance, this operating condition contains only a single MPP. A more rigorous assessment is therefore required under PSCs, where multiple local optima challenge the optimisation process.

Table 4. Statistical performance metrics of various competing under uniform dynamic condition (UDC) across 30 independent runs

Algorithm	**Tracking Efficiency (%)**	**Convergence Speed (s)**	**ITSE ($\times 10^4$)**
STC at 1000 W/m^2 ($0\ s \le t < 1.5\ s$):			
ALF-SCA	99.19 ± 3.25	0.72 ± 0.20	6.96 ± 4.59
SCA	89.98 ± 15.36	0.90±0.35	88.67 ± 38.69
PSO	99.88 ± 0.25	0.90±0.15	14.93 ± 9.54
WOA	96.53 ± 8.79	1.05±0.25	34.86 ± 14.25
HHO	91.80 ± 8.95	0.53±0.30	26.76 ± 16.14
PO	99.92	0.64	15.28
At 800 W/m^2 ($1.5\ s \le t < 3.0\ s$):			
ALF-SCA	99.71 ± 0.67	0.88 ± 0.26	7.16 ± 6.51
SCA	89.07 ± 16.28	0.70 ± 0.56	36.99 ± 30.60
PSO	98.04 ± 6.82	0.91 ± 0.24	8.60 ± 8.79
WOA	98.58 ± 3.62	1.00 ± 0.23	18.17 ± 6.79
HHO	95.73 ± 3.83	0.52 ± 0.32	13.50 ± 12.24
PO	99.92 ± 0.00	0.15 ± 0.00	0.02 ± 0.00
At 400 W/m^2 ($3.0\ s \le t \le 4.5\ s$)			
ALF-SCA	99.14 ± 3.76	0.64 ± 0.20	0.52 ± 0.67
SCA	91.78 ± 13.40	0.83 ± 0.30	8.64 ± 4.36
PSO	97.13 ± 9.69	0.85 ± 0.25	1.58 ± 1.81
WOA	98.15 ± 8.06	0.84 ± 0.22	1.85 ± 1.47
HHO	89.16 ± 10.54	0.36 ± 0.25	1.61 ± 1.07
PO	99.96 ± 0.00	0.56 ± 0.00	0.59 ± 0.00

Note: ALF-SCA = Asymmetric Leader-Follower Sine Cosine Algorithm, SCA = Sine Cosine Algorithm, PSO = Particle Swarm Optimisation, WOA = Whale Optimisation Algorithm, HHO = Harris Hawks Optimisation, PO = Perturb and Observe, ITSE = integral of time-weighted squared error, STC = Standard Test Condition.

6.2 Dynamic partial shading case 1

Following the baseline evaluation under uniform irradiance, the proposed controller was assessed under the first dynamic partial shading scenario (DPSC1), where multiple LMPPs coexist with the GMPP. This scenario evaluates the capability of each MPPT algorithm to distinguish the GMPP from neighbouring local optima while adapting to abrupt changes in irradiance distribution. DPSC1 consists of two operating conditions, namely PSC1 and PSC2, with theoretical GMPPs of 1074.52 W and 1256.62 W, respectively. The irradiance profile changes from PSC1 to PSC2 at t = 1.5 s, requiring the controller to detect the environmental change and re-establish operation at the new GMPP.

As illustrated in Figure 7, the conventional PO algorithm rapidly converged to a local maximum under both shading conditions, demonstrating the inherent limitation of hill-climbing techniques under multimodal P–V characteristics. Although the stochastic optimisation algorithms successfully explored the search space, clear differences in tracking behaviour were observed. The original SCA exhibited noticeable oscillations before stabilisation, whereas PSO, WOA, and HHO required longer convergence periods following the irradiance transition. In contrast, ALF-SCA consistently converged towards the theoretical GMPP while maintaining a smoother transient response after each environmental change.

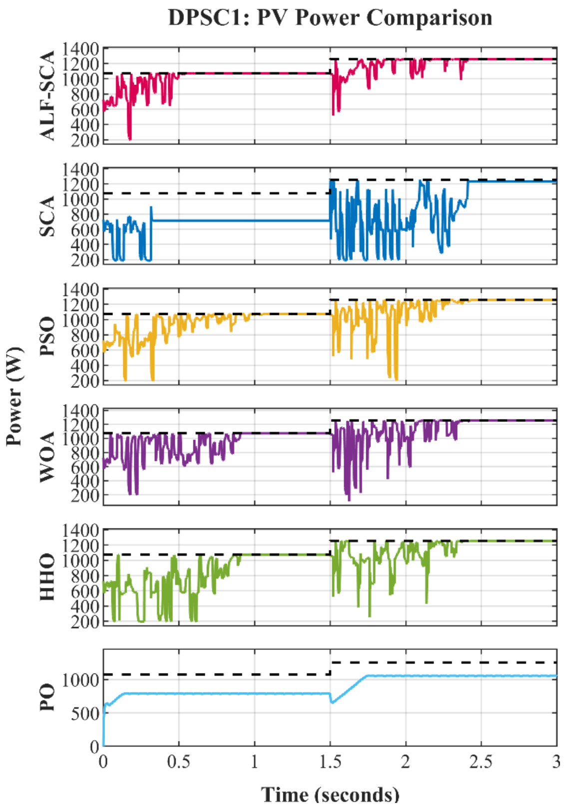

Figure 7. Time-domain photovoltaic (PV) power tracking comparison under severe dynamic partial shading transitions (DPSC1: PSC1 → PSC2)

Table 5. Statistical performance metrics of various competing algorithms under dynamic partial shading condition 1 (DPSC1) across 30 independent runs

Algorithm	Tracking Efficiency (%)	Convergence Speed (s)	ITSE ($\times 10^4$)
PSC1 ($0 \text{ s} \leq t < 1.5 \text{ s}$):			
ALF-SCA	93.53 ± 12.32	0.87 ± 0.28	2.51 ± 1.68
SCA	86.38 ± 16.69	0.93 ± 0.32	9.66 ± 3.02
PSO	96.24 ± 9.20	0.99 ± 0.27	3.01 ± 1.63
WOA	91.14 ± 12.82	1.06 ± 0.31	5.53 ± 2.15
HHO	79.17 ± 14.74	0.66 ± 0.44	5.31 ± 2.03
PO	73.62	0.14	3.30
PSC2 ($1.5 \text{ s} \leq t \leq 3.0 \text{ s}$):			
ALF-SCA	98.69 ± 4.15	0.73 ± 0.24	0.72 ± 0.47
SCA	83.26 ± 9.58	0.17 ± 0.36	3.63 ± 3.60
PSO	95.23 ± 9.88	0.84 ± 0.40	2.30 ± 2.45
WOA	94.20 ± 7.93	0.61 ± 0.47	2.37 ± 1.85
HHO	92.62 ± 11.67	0.43 ± 0.36	2.74 ± 3.61
PO	83.96	0.24	1.90

Note: ALF-SCA = Asymmetric Leader-Follower Sine Cosine Algorithm, SCA = Sine Cosine Algorithm, PSO = Particle Swarm Optimisation, WOA = Whale Optimisation Algorithm, HHO = Harris Hawks Optimisation, PO = Perturb and Observe, ITSE = integral of time-weighted squared error, PSC = partial shading condition.

The statistical results presented in Table 5 further validate these observations. Under PSC2, ALF-SCA achieved the highest mean tracking efficiency (98.69 ± 4.15%) together with the lowest ITSE (0.72 ± 0.47) among the stochastic optimisation algorithms. In comparison, the original SCA recorded a lower tracking efficiency (83.26 ± 9.58%) and a significantly larger ITSE (3.63 ± 3.60), indicating poorer convergence stability. These results demonstrate that ALF-SCA maintains accurate and repeatable GMPP tracking under dynamic partial shading while substantially reducing cumulative tracking errors.

The improved performance achieved under DPSC1 indicates that the proposed controller can reliably recover from abrupt irradiance changes without becoming trapped at neighbouring local optima. To further examine its robustness, the next evaluation considers a substantially more challenging operating condition containing a larger number of competing power peaks.

6.3 Dynamic partial shading case 2

The final evaluation was conducted under Dynamic partial shading condition 2 (DPSC2), which represents the most challenging operating scenario considered in this study. Compared with DPSC1, this scenario introduces increasingly complex multimodal P–V characteristics, including a severe partial shading profile with twelve distinct power peaks. Consequently, the optimisation algorithm must accurately distinguish the GMPP from numerous neighbouring local optima while maintaining rapid convergence following abrupt environmental changes. The two operating conditions, PSC3 and PSC4, have theoretical GMPPs of 1985.44 W and 924.94 W, respectively.

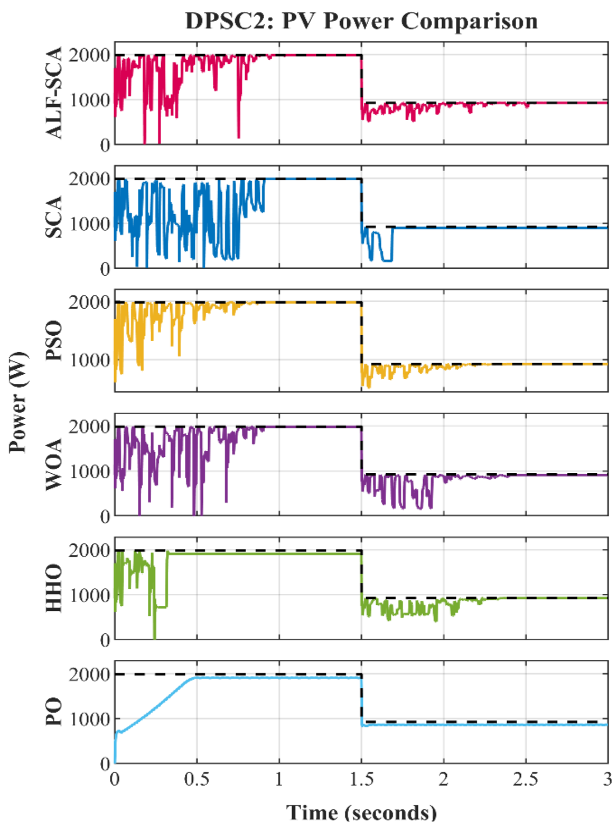

Figure 8. Time-domain photovoltaic (PV) power tracking comparison under severe dynamic partial shading transitions (DPSC2: PSC3 → PSC4)

The transient responses shown in Figure 8 demonstrate that the proposed ALF-SCA maintained stable tracking performance throughout both operating conditions. Under PSC3, all metaheuristic-based algorithms successfully approached the GMPP; however, the original SCA exhibited noticeable oscillations before reaching steady state, whereas WOA and HHO required longer convergence periods. Following the transition to PSC4 at t = 1.5 s, the optimisation landscape became considerably more complex because of the twelve competing power peaks. Under this condition, PO again converged to a local optimum, while the original SCA and other benchmark metaheuristic experienced larger transient fluctuations before stabilisation. In comparison, ALF-SCA rapidly converged to the new GMPP while maintaining a comparatively smooth power response throughout the remaining simulation period.

The statistical results summarised in Table 6 further confirm the robustness of the proposed controller. ALF-SCA achieved mean tracking efficiencies of 99.91 ± 0.22% under PSC3 and 99.84 ± 0.48% under PSC4, while consistently producing the lowest ITSE among the evaluated stochastic optimisation algorithms. Under PSC4, the ITSE was reduced to 0.12 ± 0.07, substantially lower than that obtained by the original SCA (4.55 ± 2.35). These results demonstrate that the proposed controller maintains excellent tracking accuracy, rapid convergence, and stable operation even under highly complex PSCs characterised by multiple competing local optima.

Table 6. Statistical performance metrics of various competing algorithm under dynamic partial shading condition 2 (DPSC2) across 30 independent runs

Algorithm	Tracking Efficiency (%)	Convergence Speed (s)	ITSE ($\times 10^4$)
PSC3 (0 s ≤ t < 1.5 s):			
ALF-SCA	99.91 ± 0.22	0.77 ± 0.18	2.23 ± 1.94
SCA	98.82 ± 0.87	0.82 ± 0.24	43.11 ± 18.29
PSO	99.90 ± 0.25	0.87 ± 0.07	4.65 ± 3.84
WOA	99.62 ± 0.74	0.99 ± 0.22	11.76 ± 4.89
HHO	98.63 ± 1.23	0.51 ± 0.36	9.31 ± 9.22
PO	96.10	0.48	4.57
PSC4 (1.5 s ≤ t ≤ 3.0 s):			
ALF-SCA	99.84 ± 0.48	0.73 ± 0.14	0.12 ± 0.07
SCA	97.55 ± 1.02	0.81 ± 0.27	4.55 ± 2.35
PSO	99.83 ± 0.37	0.90 ± 0.13	0.38 ± 0.27
WOA	99.60 ± 0.72	0.96 ± 0.15	1.20 ± 0.58
HHO	98.15 ± 1.61	0.46 ± 0.34	0.66 ± 0.66
PO	93.28	0.06	0.16

Note: ALF-SCA = Asymmetric Leader-Follower Sine Cosine Algorithm, SCA = Sine Cosine Algorithm, PSO = Particle Swarm Optimisation, WOA = Whale Optimisation Algorithm, HHO = Harris Hawks Optimisation, PO = Perturb and Observe, ITSE = integral of time-weighted squared error, PSC = partial shading condition.

7. DISCUSSION

The superior performance of the proposed ALF-SCA is not attributed to a single modification but to the coordinated integration of four complementary design components, namely the asymmetric leader-follower update strategy, global-best anchoring, convergence locking criterion, and environmental reinitialisation mechanism. Together, these components improve the balance between exploration and exploitation while preserving convergence stability under dynamic operating conditions. The experimental results presented in Section 6 consistently demonstrate that these design decisions enable ALF-SCA to maintain high tracking accuracy with reduced transient oscillations across increasingly complex PV operating scenarios.

7.1 Design rationale and performance analysis

A key design feature of the proposed framework is the asymmetric assignment of the destination weight, r_3, to the leader and follower agents. Unlike the standard SCA, where all agents update their positions using stochastic destination weights, ALF-SCA assigns a stochastic destination weight ($r_3 \in [0, 2]$) only to the leader agent, while the follower agents employ a fixed destination weight ($r_3 = 1$). This asymmetric update strategy allows the leader to continue exploring the neighbourhood of the current best solution while directing the followers towards the identified global-best position. Consequently, exploration is preserved without maintaining unnecessary population diversity during the later stages of optimisation.

The global-best anchoring strategy further complements this behaviour by providing a common reference for population movement. Instead of allowing individual agents to evolve independently throughout the optimisation process, the follower population progressively contracts towards the best solution identified by the leader. This coordinated search mechanism accelerates convergence while reducing duty-cycle fluctuations after the GMPP has been identified. The improvement is evident from the consistently lower ITSE values and smoother transient responses observed under both uniform irradiance and PSCs.

Another important component is the convergence locking criterion, which prevents unnecessary position updates once the population has converged. Conventional population-based MPPT algorithms often continue perturbing the operating duty cycle after reaching the optimum solution, resulting in persistent steady-state oscillations. In contrast, ALF-SCA terminates the optimisation process once the convergence criterion is satisfied and maintains the optimum duty cycle until a significant environmental change is detected. This strategy contributes directly to the improved steady-state stability observed throughout the experimental evaluation.

Finally, the environmental reinitialisation mechanism enables continuous adaptation under dynamic irradiance conditions. Rather than remaining at the previously identified operating point, the optimisation process is automatically restarted whenever a significant change in the PV operating condition is detected. This adaptive behaviour allows the controller to rapidly identify the new GMPP following irradiance transitions, contributing to the consistently high tracking efficiencies achieved under both DPSC1 and DPSC2.

Collectively, these four design components operate as a unified optimisation framework rather than independent modifications. Their combined effect enables ALF-SCA to maintain an effective balance between exploration, exploitation, convergence stability, and dynamic adaptability, thereby explaining the consistent performance improvements observed over the benchmark MPPT algorithms.

7.2 Computational efficiency, practical implications, and study limitations

Although ALF-SCA introduces additional coordination through the asymmetric leader-follower strategy and convergence control mechanism, these modifications do not increase the theoretical computational complexity of the original SCA. As summarised in Table 7, both algorithms retain the same computational complexity from the Big O notation, while the measured execution latency of ALF-SCA increases only marginally compared with the standard SCA. This indicates that the proposed framework improves tracking performance through a more effective search strategy rather than increased computational effort.

Table 7. Computational complexity and execution latency of the evaluated MPPT algorithms

Algorithm	Time Complexity	Measured Active Sampling Latency (μs)
Proposed ALF-SCA	$O(N \cdot D)$	5.4029
SCA	$O(N \cdot D)$	5.1582
PSO	$O(N \cdot D)$	6.7194
WOA	$O(N \cdot D)$	6.8466
HHO	$O(N \cdot D)$	6.0170
PO	$O(1)$	1.5309

Note: *Measured active sampling latency represents the average physical execution time per sampling iteration ($T_s = 15$ ms), calculated over 10^4 (10,000) consecutive sampling loops using MATLAB system timers (tic/toc) to eliminate operating system background noise. MPPT = maximum power point tracking, ALF-SCA = Asymmetric Leader-Follower Sine Cosine Algorithm, SCA = Sine Cosine Algorithm, PSO = Particle Swarm Optimisation, WOA = Whale Optimisation Algorithm, HHO = Harris Hawks Optimisation, PO = Perturb and Observe.

Moreover, from a practical implementation perspective, the measured execution latency remains significantly lower than the adopted MPPT sampling interval, confirming that the proposed MPPT does not introduce computational overhead.

The combination of high tracking efficiency reduced steady-state oscillation, and low computational overhead makes ALF-SCA a practical candidate for dynamic MPPT applications where both tracking performance and computational efficiency are equally important.

The present study is limited to simulation-based validation under varying irradiance conditions using MATLAB which are not sufficient as a complete validation of the proposed work. Although the proposed controller demonstrated consistent performance under progressively more challenging operating scenarios, further validation using hardware implementation or HIL platforms would provide additional verification of its practical applicability. Future work will also investigate the robustness of ALF-SCA under simultaneous irradiance, temperature, and load variations.

8. CONCLUDING REMARK

This paper proposed ALF-SCA for GMPPT of PV systems operating under dynamic PSCs. The proposed framework integrates four complementary design components, namely asymmetric leader-follower coordination, global-best anchoring, convergence locking, and environmental reinitialization, to improve the balance between exploration and exploitation while maintaining convergence stability. Unlike the standard SCA, the proposed strategy enhances population coordination without increasing the theoretical computational complexity, making it suitable for real-time MPPT applications.

The effectiveness of ALF-SCA was comprehensively evaluated under progressively challenging operating conditions, including uniform dynamic irradiance and two dynamic partial shading scenarios. The experimental results demonstrated that the proposed controller consistently achieved high tracking efficiency with lower cumulative tracking errors and smoother transient responses than the benchmark algorithms. In particular, the proposed framework maintained reliable GMPP tracking under highly multimodal P-V characteristics while exhibiting improved optimisation repeatability and reduced steady-state oscillations. Furthermore, the computational analysis confirmed that these performance improvements were achieved with only a marginal increase in execution latency, supporting the practical feasibility of the proposed approach.

Overall, the proposed ALF-SCA provides an effective and computationally efficient solution for dynamic MPPT in PV systems. Future work will focus on experimental validation using embedded hardware platforms and on extending the proposed framework to evaluate its robustness under simultaneous irradiance, temperature, and load variations.

ACKNOWLEDGEMENT

This work has been funded by the Distinguished Research Grant Scheme under the university reference number RDU253302. This grant has been conferred by the Research and Innovation Division, Universiti Malaysia Pahang Al-Sultan Abdullah.

REFERENCES

[1] Kumar, H., Khurana, N., Pareek, S. (2025). Enhancing the performance of solar panel during partial shedding condition. Darpan International Research Analysis, 13(2): 15-39. https://doi.org/10.36676/dira.v13.i2.166

[2] Mamun, M.A.A., Hasanuzzaman, M., Selvaraj, J. (2017). Experimental investigation of the effect of partial shading on photovoltaic performance. IET Renewable Power Generation, 11(7): 912-921. https://doi.org/10.1049/iet-rpg.2016.0902

[3] Bhos, C., Nasikkar, P. (2024). Mitigation of power losses in solar photovoltaic systems under partial shading using optimization-based MPPT. Journal Européen des Systèmes Automatisés, 57(6): 1621-1630. https://doi.org/10.18280/jesa.570609

[4] Sadick, A. (2023). Maximum power point tracking simulation for photovoltaic systems using perturb and observe algorithm. In Solar Radiation-Enabling Technologies, Recent Innovations, and Advancements for Energy Transition. IntechOpen. https://doi.org/10.5772/intechopen.111632

[5] Ahmed, J., Salam, Z. (2015). An improved perturb and observe (P&O) maximum power point tracking (MPPT) algorithm for higher efficiency. Applied Energy, 150: 97-108. https://doi.org/10.1016/j.apenergy.2015.04.006

[6] Jabbar, R.I., Mekhilef, S., Mubin, M., Mohammed, K.K. (2023). A modified perturb and observe MPPT for a fast and accurate tracking of MPP under varying weather conditions. IEEE Access, 11: 76166-76176. https://doi.org/10.1109/ACCESS.2023.3297445

[7] Ji, R., Wang, Z. (2023). Improved variable-step incremental conductance MPPT algorithm applied to photovoltaic storage systems. Journal of Physics: Conference Series, 2427(1): 012045. https://doi.org/10.1088/1742-6596/2427/1/012045

[8] Ibrahim, M.H., Ang, S.P., Dani, M.N., Rahman, M.I., Petra, R., Sulthan, S.M. (2023). Optimizing step-size of perturb & observe and incremental conductance MPPT techniques using PSO for grid-tied PV system. IEEE Access, 11: 13079-13090.

https://doi.org/10.1109/ACCESS.2023.3242979
[9] Ahmed, J., Salam, Z. (2018). An enhanced adaptive P&O MPPT for fast and efficient tracking under varying environmental conditions. IEEE Transactions on Sustainable Energy, 9(3): 1487-1496. https://doi.org/10.1109/TSTE.2018.2791968
[10] Hashim, N., Salam, Z. (2019). Critical evaluation of soft computing methods for maximum power point tracking algorithms of photovoltaic systems. International Journal of Power Electronics and Drive Systems, 10(1): 548-561. https://doi.org/10.11591/ijpeds.v10.i1.pp548-561
[11] Naser, A.T., Mohammed, K.K., Ab Aziz, N.F., binti Kamil, K., Mekhilef, S. (2024). Improved coot optimizer algorithm-based MPPT for PV systems under complex partial shading conditions and load variation. Energy Conversion and Management: X, 22: 100565. https://doi.org/10.1016/j.ecmx.2024.100565
[12] Zeddini, M.A., Krim, S., Mansouri, M., Mimouni, M.F., Sakly, A. (2024). Fuzzy logic adaptive crow search algorithm for MPPT of a partially shaded photovoltaic system. IEEE Access, 12: 119246-119271. https://doi.org/10.1109/ACCESS.2024.3434523
[13] Khan, N.M., Khan, U.A., Asif, M., Zafar, M.H. (2024). Analysis of deep learning models for estimation of MPP and extraction of maximum power from hybrid PV-TEG: A step towards cleaner energy production. Energy Reports, 11: 4759-4775. https://doi.org/10.1016/j.egyr.2024.04.035
[14] Velasco, L., Guerrero, H., Hospitaler, A. (2024). A literature review and critical analysis of metaheuristics recently developed. Archives of Computational Methods in Engineering, 31(1): 125-146. https://doi.org/10.1007/s11831-023-09975-0
[15] Sedik, K.M., Attia, M.A., Abdelaziz, A.Y., Sameh, M.A. (2026). Maximum power point tracking in PV systems and partial shading: A review. Journal of Physics: Conference Series, 3191(1): 012070. https://doi.org/10.1088/1742-6596/3191/1/012070
[16] Jabbar, R.I., Mekhilef, S., Mubin, M., Wahyudie, A. (2025). A high-performance hybrid MPPT method for rapid tracking and steady power operation under varying weather conditions and load changes in photovoltaic systems. IEEE Access, 13: 153072-153092. https://doi.org/10.1109/ACCESS.2025.3603641
[17] Venugopal, M., Mahadevaswamy, M., Gowri, M.B.S. (2025). Intelligent maximum power point tracking control for solar photovoltaic systems using fuzzy and neuro-fuzzy techniques. Bulletin of Electrical Engineering and Informatics, 14(6): 4290-4303. https://doi.org/10.11591/eei.v14i6.10735
[18] Ishaque, K., Salam, Z. (2013). A deterministic particle swarm optimization maximum power point tracker for photovoltaic system under partial shading condition. IEEE Transactions on Industrial Electronics, 60(8): 3195-3206. https://doi.org/10.1109/TIE.2012.2200223
[19] Zhang, X., Zhao, B., Cui, H., Zhao, G., Li, Y., Huangfu, Y. (2025). A hybrid global maximum power point tracking control method based on particle swarm optimization (PSO) and perturbation and observation (P&O). Electric Power Systems Research, 248: 111967. https://doi.org/10.1016/j.epsr.2025.111967
[20] Refaat, A., Khalifa, A.E., Elsakka, M.M., Elhenawy, Y., Kalas, A., Elfar, M.H. (2023). A novel metaheuristic MPPT technique based on enhanced autonomous group particle swarm optimization algorithm to track the GMPP under partial shading conditions-experimental validation. Energy Conversion and Management, 287: 117124. https://doi.org/10.1016/j.enconman.2023.117124
[21] Laxman, B., Annamraju, A., Srikanth, N.V. (2021). A grey wolf optimized fuzzy logic based MPPT for shaded solar photovoltaic systems in microgrids. International Journal of Hydrogen Energy, 46(18): 10653-10665. https://doi.org/10.1016/j.ijhydene.2020.12.158
[22] Mohanty, S., Subudhi, B., Ray, P.K. (2016). A new MPPT design using grey wolf optimization technique for photovoltaic system under partial shading conditions. IEEE Transactions on Sustainable Energy, 7(1): 181-188. https://doi.org/10.1109/TSTE.2015.2482120
[23] Ahessab, H., Gaga, A., El Hadadi, B. (2025). Revolutionizing photovoltaic power: An enhanced Grey Wolf Optimizer for ultra-efficient MPPT under partial shading conditions. Scientific African, 27: e02586. https://doi.org/10.1016/j.sciaf.2025.e02586
[24] Karmouni, H., Chouiekh, M., Motahhir, S., Qjidaa, H., Jamil, M.O., Sayyouri, M. (2022). A fast and accurate sine-cosine MPPT algorithm under partial shading with implementation using arduino board. Cleaner Engineering and Technology, 9: 100535. https://doi.org/10.1016/j.clet.2022.100535
[25] Chandrasekaran, K., Sankar, S., Banumalar, K. (2020). Partial shading detection for PV arrays in a maximum power tracking system using the sine-cosine algorithm. Energy for Sustainable Development, 55: 105-121. https://doi.org/10.1016/j.esd.2020.01.007
[26] Padmanaban, S., Priyadarshi, N., Holm-Nielsen, J.B., 二 et al. (2019). A novel modified sine-cosine optimized MPPT algorithm for grid integrated PV system under real operating conditions. IEEE Access, 7: 10467-10477. https://doi.org/10.1109/ACCESS.2018.2890533
[27] Bettahar, F., Abdeddaim, S., Betka, A. (2025). Hardware-in-the-loop implementation of the hybrid FPA-P&O approach for optimizing photovoltaic systems under partial shading conditions. Journal of Renewable Energies, 28(1): 169-185. https://doi.org/10.54966/jreen.v28i1.1279
[28] Al-Hussein, A.B.A., Tahir, F.R., Pham, V.T. (2025). FPGA implementation of synergetic controller-based MPPT algorithm for a standalone PV system. Computation, 13(3): 64. https://doi.org/10.3390/computation13030064
[29] Mirjalili, S. (2016). SCA: A sine cosine algorithm for solving optimization problems. Knowledge-Based Systems, 96: 120-133. https://doi.org/10.1016/j.knosys.2015.12.022
[30] Hassan, A., Bass, O., Masoum, M.A.S. (2023). An improved genetic algorithm based fractional open circuit voltage MPPT for solar PV systems. Energy Reports, 9: 1535-1548. https://doi.org/10.1016/j.egyr.2022.12.088
[31] Mirza, A.F., Mansoor, M., Ling, Q., Yin, B., Javed, M.Y. (2020). A SALP-swarm optimization based MPPT technique for harvesting maximum energy from PV systems under partial shading conditions. Energy Conversion and Management, 209: 112625. https://doi.org/10.1016/j.enconman.2020.112625
[32] Villalva, M.G., Gazoli, J.R., Ruppert Filho, E. (2009). Comprehensive approach to modeling and simulation of photovoltaic arrays. IEEE Transactions on Power

Electronics, 24(5): 1198-1208. https://doi.org/10.1109/TPEL.2009.2013862
[33] Shams, I., Mekhilef, S., Tey, K.S. (2021). Improved-team-game-optimization-algorithm-based solar MPPT with fast convergence speed and fast response to load variations. IEEE Transactions on Industrial Electronics, 68(8): 7093-7103. https://doi.org/10.1109/TIE.2020.3001798
[34] Mohammed, K.K., Mekhilef, S. (2024). Improved snake optimizer algorithm-based GMPPT with a fast response to the load variations under different weather conditions for PV systems. IEEE Transactions on Industrial Electronics, 71(7): 7147-7157. https://doi.org/10.1109/TIE.2023.3301526
[35] Eltamaly, A.M. (2021). A novel musical chairs algorithm applied for MPPT of PV systems. Renewable and Sustainable Energy Reviews, 146: 111135. https://doi.org/10.1016/j.rser.2021.111135
[36] Yao, X., Liu, Y., Lin, G. (1999). Evolutionary programming made faster. IEEE Transactions on Evolutionary Computation, 3(2): 82-102. https://doi.org/10.1109/4235.771163
[37] Ishaque, K., Salam, Z., Amjad, M., Mekhilef, S. (2012). An improved particle swarm optimization (PSO)-based MPPT for PV with reduced steady-state oscillation. IEEE Transactions on Power Electronics, 27(8): 3627-3638. https://doi.org/10.1109/TPEL.2012.2185713
[38] Mirjalili, S., Lewis, A. (2016). The Whale Optimization Algorithm. Advances in Engineering Software, 95: 51-67. https://doi.org/10.1016/j.advengsoft.2016.01.008
[39] Mansoor, M., Mirza, A.F., Ling, Q. (2020). Harris hawk optimization-based MPPT control for PV systems under partial shading conditions. Journal of Cleaner Production, 274: 122857. https://doi.org/10.1016/j.jclepro.2020.122857

NOMENCLATURE

I	Photovoltaic current
V	Photovoltaic voltage
P	Photovoltaic power
V_{mp}	Voltage at the maximum power point
I_{mp}	Current at maximum power point
d_k^t	Duty cycle (position) of agent k at iteration t
d^*	Global best duty cycle
d_{min} $/d_{max}$	Minimum and maximum duty cycle limits
r_1	Step size control parameter
r_2	Random radian parameter in [0, 2π]
r_3	Destination weight or stochastic weight
r_4	Probability rate for sine/cosine selection
a	Initial value for the linear reduction of r_1
t	Current iteration
T	Maximum number of iterations
P_{ratio}	Power ratio for environmental change detection
ΔV	Change in voltage between iterations
ΔI	Change in current between iterations
Δd_{th}	Population diversity or duty cycle variance threshold